Research Article | Vol. 12, No. 10 / 1 Oct 2021 / Biomedical Optics Express 6590
Biomedical Optics EXPRESS

Real-time monitoring of the sucrose hydrolysis process based on two-photon coincidence measurements

ZHENG PENG,[1] ZHIYUAN ZHOU,[2] TONGJU LI,[1] MEILI JIANG,[1] CHENHAO LI,[1] TANG QING,[1,3] LIU YANG,[1] AND XIAOCHUN ZHANG[1,*]

[1]ENNOVA Institute of Life Science and Technology, ENN Group, Langfang, Hebei 065001, China
[2]CAS Key Laboratory of Quantum Information, University of Science and Technology of China, Hefei, Anhui 230026, China
[3]College of Physics, Sichuan University, Chengdu, Sichuan 610064, China
*zhangxcb@enn.cn

Abstract: Real-time measurement of the biochemical reaction process has important application scenarios. Due to the chirality of a large number of life-sustaining molecules, many parameters of the reaction kinetics involving these chiral molecules, such as the reaction rate and the reagents concentrations, could be tracked by monitoring the optical activity of the substrate and/or product molecules. However, the optical activity of photosensitive biomolecules does not allow traditional laser-based real-time measurement due to the vulnerability of their biochemical properties under high-intensity light regimes. Here we introduce a real-time tracking technique of the sucrose hydrolysis reaction based on two-photon coincidence measurements. The two-photon source is generated based on a spontaneous parametric down-conversion process. During the reaction, the kinetic parameters are obtained by the real-time measurement of the change of the polarization of the photons when operating at extremely low-light regimes. Compared with single-photon counting measurements, two-photon coincidence measurements have higher signal-to-noise ratios and better robustness, which demonstrates the potential value in monitoring the photosensitive biochemical reaction processes.

1. Introduction

Many biological proteins, enzymes, and small energy metabolism molecules are chiral in structure, with their chirality leading to a rotation of the plane of the in-coming polarized light, which is the optical activity of the chiral molecules. Molecules with different optical activities can be used to identify the 3D structures of these molecules [1]. By tracking the change of the reagents optical activity, real-time measurement of the kinetic parameters of biochemical reaction processes, in which chiral molecules participate, can be performed. Thus, evaluation of enzyme activity can also be achieved [2]. For industrial production, long-term monitoring of biochemical reaction processes is often required, hence the use of optical activity tracking methods in industrial applications is also a meaningful technique.

Since many biomolecules are photosensitive, long-time exposure to a traditional polarized laser beam will inevitably affect the reaction process [3,4]. The weaker the light, the less influence the reaction will suffer. However, when an extremely weak beam is applied, the impact of shot noise [5–7], becomes the main factor compromising the accuracy and precision of the measurement. In the low-light regime, the fluctuation of the photon flux and the influence of environmental noise become more relevant, hence quantum correlation measurements can be applied to effectively eliminate the influence of environmental noise [8–11], thereby improving the signal-to-noise ratio of the measurement.

#432301 https://doi.org/10.1364/BOE.432301
Journal © 2021 Received 30 Jul 2021; revised 10 Sep 2021; accepted 17 Sep 2021; published 30 Sep 2021

Biomedical Optics EXPRESS

With the rapid development of quantum theory and technology, the advantages of quantum metrology [12–15] for biological research and future sensors have received great attention for the reasons below: single-photon level measurements and measurements based on quantum entangled states can extract extremely weak signals from the complex noise background. Quantum measurements based on multiple-photon states also enjoy the characteristics of ultra-high resolution and ultra-sensitivity [13,15]. An another area of active research exploiting the quantum optical feature of induced coherence also attracts great interest by using the most sensitive light band (visible light to near-infrared) to explore signals generated by other electromagnetic bands [16–18]. Among the related works, A. V. Paterova et al. studied the phase retardation introduced by a birefringent sample in the infrared range based on the interference effect of frequency nondegenerate spontaneous parametric down conversion (SPDC) [19], which is also polarization measurement as introduced in this article but pushed the polarimetry technique to the IR region. In addition to operating at a single wavelength, some recent works based on the effect of nonlinear interference of correlated photons [20–23] have demonstrated its power in hyperspectral infrared microscopy with high spatial resolution and fast readout speed and will find their way into the applications in biological studies in the future.

Bio-chiral molecules are optically active and have circularly polarized birefringence, therefore the change in the component concentrations of a biochemical reaction can be dynamically tracked by monitoring the optical activities of the reagents [24–27]. Classical polarization measurements and interferometric methods are usually performed to monitor the above characteristics. Since long-term exposure to strong light may well affect properties of the reactants/products or the progress of the reaction, using ultra-weak quantum light to monitor the process of biochemical reactions has its unique advantages: First, consider the use of ultra-weak power. For example, a general quantum level light source has about 10^6 count per second (cps) incident photons, which is equivalent to 10^{-13} W, thus imposing minimal invasiveness on biomolecules. In addition, the correlation between photons can effectively eliminate the influence of external noise, resulting in a higher signal-to-noise ratio and better robustness compared with direct single-photon measurements.

This article introduces a method that applies the coincidence measurement of the polarization state of a labeled photon to calculate the concentration of various reagent molecules in the reaction process of a chiral bio-molecular solution over time. Using a two-photon light source with high brightness and high coincidence count rate as our quantum probe, the hydrolysis process of sucrose to glucose under the catalysis of dilute hydrochloric acid is measured in real time. Comparing the result with that obtained from the classical single-photon measurement method, it is found that the method based on two-photon coincidence measurement has a better signal-to-noise ratio and is less sensitive to changes in ambient light.

2. Methods

2.1. Basic principles

Generally, biomolecules with chirality are optically active. Sucrose and glucose are right-handed molecules, and fructose is left-handed. Their specific rotations at the wavelength of 800nm and the temperature of 20°C are:

$$[\alpha]_{800}^{20} = +34.84^\circ \text{ (sucrose)}$$
$$[\alpha]_{800}^{20} = +28.04^\circ \text{ (d - glucose)}$$
$$[\alpha]_{800}^{20} = -48.70^\circ \text{ (d - fructose)}$$

Adding a certain amount of hydrochloric acid to the sucrose solution will cause a hydrolysis reaction:

$$C_{12}H_{22}O_{11}(\text{sucrose}) + H_2O \rightarrow C_6H_{12}O_6(\text{glucose}) + C_6H_{12}O_6(\text{fructose})$$

Biomedical Optics EXPRESS

Due to the difference in the optical activities of sucrose, glucose and fructose, the changes in the optical rotation of the solution can be used to extract the real-time concentration changes of the three components during the reaction process. For convenience, we convert the above three specific optical rotations into molar concentration units. Using the molecular weight of sucrose (342.297) as well as these of glucose and fructose (both 180.16), we get the specific molar rotations:

$$[\alpha]_{\mathrm{S}}^{\mathrm{mol}} = +11.92^{\circ}\mathrm{L}(\mathrm{mol}^{-1}\mathrm{dm}^{-1}) \text{ (sucrose)}$$

$$[\alpha]_{\mathrm{G}}^{\mathrm{mol}} = +5.05^{\circ}\mathrm{L}(\mathrm{mol}^{-1}\mathrm{dm}^{-1}) \text{ (d - glucose)}$$

$$[\alpha]_{\mathrm{F}}^{\mathrm{mol}} = -8.77^{\circ}\mathrm{L}(\mathrm{mol}^{-1}\mathrm{dm}^{-1}) \text{ (d - fructose)}$$

Suppose that the molar concentrations of sucrose, glucose and fructose in the reaction process changes with time as: $C_{\mathrm{S}}(t)$, $C_{\mathrm{G}}(t)$ and $C_{\mathrm{F}}(t)$. Then we have:

$$C_{\mathrm{G}}(t) = C_{\mathrm{S}}(0) - C_{\mathrm{S}}(t) \tag{1}$$

$$C_{\mathrm{F}}(t) = C_{\mathrm{S}}(0) - C_{\mathrm{S}}(t) \tag{2}$$

where $C_{\mathrm{S}}(0)$ is the initial concentration of sucrose and $C_{\mathrm{S}}(t)$ is the concentration at time t. Therefore, with a given sample tube length of 5cm, the total optical rotation is:

$$\alpha_{\mathrm{T}}(t) = 0.5(C_{\mathrm{S}}(t) \cdot [\alpha]_{\mathrm{S}}^{\mathrm{mol}} + C_{\mathrm{G}}(t) \cdot [\alpha]_{\mathrm{G}}^{\mathrm{mol}} + C_{\mathrm{F}}(t) \cdot [\alpha]_{\mathrm{F}}^{\mathrm{mol}}) \tag{3}$$

According to the three linear independent Eqs. (1), (2) and (3), since $C_{\mathrm{S}}(0)$ is obtained from the initial state, if α_{T} (t) is measured, then we can get unique values for the three unknowns $C_{\mathrm{S}}(t)$, $C_{\mathrm{G}}(t)$ and $C_{\mathrm{F}}(t)$ by calculation.

2.2. Optical scheme and layout

Figure 1 is the schematic diagram of the layout for the optical measurements. The 400nm (maximum 50mW) laser beam output from the semiconductor laser goes through the λ/2 wave plate (WP1) and λ/4 wave plate (used to adjust the pump intensity) and is incident on the polarization beamsplitter (PBS1). The horizontally polarized light passing through PBS1 is reflected by an off-axis parabolic mirror (M2) and focuses on the center position of the ppKTP (periodically poled potassium titanyl phosphate) crystal (polarization period of 10.02 μm) with type-II phase matching. The beam then triggers the SPDC process which results in a pair of horizontally (signal photon) and vertically (idler photon) polarized photons with mutually perpendicular polarizations. The frequencies of the two SPDC photons are degenerate with identical wavelengths of 800nm (although frequency degeneration is not required for this measurement). The filter (F1) is used to filter out the 400nm pump light. When the orthogonally polarized photon pair goes through the second polarization beamsplitter (PBS2), the horizontally polarized photon passes through, and the vertically polarized photon reflects into the multimode fiber, then collected by the single-photon detector D3 (SPCM-AQRH-16X manufactured by Excelitas Technology, Canada). Meanwhile, the horizontally polarized photon is incident on the transparent quartz sample cell to be measured (optical path of 5cm), and then the outgoing light goes through another high-precision λ/2 wave plate(WP2) incident on the third polarization beam splitter(PBS3). PBS3 divides the signal light (with the extra phase angle contributed by the sample solution) into two paths, then the divided beams enter two single-photon detectors D1 and D2 respectively, through multimode fiber coupling. Then the photon counting measurements, as well as coincidence counting measurements, are performed using signals from D1, D2 and D3.

Before the 800nm entangled photons enter the coupling fibers of the three single-photon detectors (D1, D2, and D3), three 800nm narrow-band pass filters F2, F3 and F4 are set respectively to filter out stray photons as much as possible. The photon-counts signal generated

Biomedical Optics EXPRESS

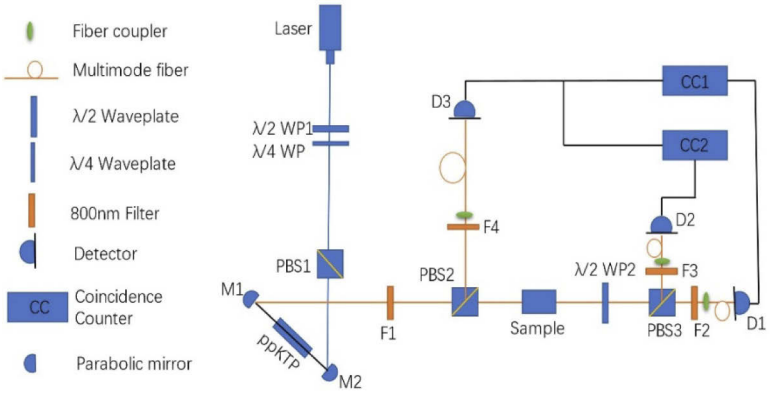

Fig. 1. Optical schematic diagram for the solution optical rotation measurement.

by D3 is branched and sent to two signal ports corresponding to the two coincidence counters (CC1, manufactured by Asky Quantum, China and CC2 TimeHarp 260, manufactured by PicoQuant, Germany) respectively. The photon-counts signal of detector D1 is connected to the synchronization port of CC1, while that of detector D2 feeds to the synchronization port of CC2.

The number of photons per second detected by D3, $I_{1\text{signal}}$ (we call it $I_{1\text{signal}}$ because it is fed to the signal port of CC1) and the number of photons per second detected by D1, $I_{1\text{sync}}$ (we call it $I_{1\text{sync}}$ because it is fed to the synchronization port of CC1) are the two input signals go into the first coincidence counter (CC1). The output of CC1 is the number of coincidences in a 3.2 ns time window of the two input signals, denoted as $I_{1\text{cc}}$. The corresponding three values of the other coincidence counter (CC2) are $I_{2\text{signal}}$ (which is equal to $I_{1\text{signal}}$ since they both come from D3), $I_{2\text{sync}}$ (from D2) and the coincidence count rate $I_{2\text{cc}}$.

After a pump photon going through the SPDC process and splitting into a photon pair, a two-photon state $|V\rangle|H\rangle$ is formed and after time evolution it becomes:

$$|V\rangle|H\rangle \rightarrow |V\rangle_3(\cos(\theta - \alpha_T(t))|H\rangle_1 + \sin(\theta - \alpha_T(t))|V\rangle_2)$$

where θ is the angle between the principal axis of the λ/2 wave plate (WP2) and the horizontal direction, which can be set in advance, $\alpha_T(t)$ is the optical rotation angle of the sample.

The photon going through the sample solution and the second λ/2 wave plate (WP2) accumulates a phase angle relative to its original horizontally polarized direction, the angle can be calculated in two different ways:

(1) Single-photon counting method:

$$\alpha = \arccos\left(\sqrt{\frac{I_{1\text{sync}}}{I_{1\text{sync}} + I_{2\text{sync}}}}\right) \tag{4}$$

(2) Two-photon coincidence counting method:

$$\alpha = \arccos\left(\sqrt{\frac{I_{1\text{cc}}}{I_{1\text{cc}} + I_{2\text{cc}}}}\right) \tag{5}$$

where $\alpha = \theta$-$\alpha_T(t)$ in the above two equations.

Therefore, if θ can be determined, the optical rotation angle $\alpha_T(t)$ of the sample can be calculated according to the corresponding photon-counts/coincidence-counts change over time.

Biomedical Optics EXPRESS

We compare the single-photon counting method with two-photon coincidence counting method using the analytic tools developed by [11].

Let x_1, x_2, and x_3 denote the quantum efficiencies of the optical channels from the generation of photon pairs to the corresponding photon detector D1, D2, and D3, then $I_{1\text{signal}} = I_{2\text{signal}} = x_3 P$, which is the number of photon-counts of D3, where P is the number of photon pairs generated from the ppKTP crystal. Similarly, the number of photon-counts of D1 is $I_{1\text{sync}} = x_1 P$ and that of D2 is $I_{2\text{sync}} = x_2 P$. Here we have included the transmission and reflection coefficients of PBS3 in x_1 and x_2 respectively. Following [11], the coincidence count rate of CC1 is:

$$I_{1\text{cc}} = x_1 x_3 P \tag{6}$$

According to [11], the number of noise coincidences of CC1, denoted as $I_{1\text{ccNoise}}$, has three contributors, which are the accidental overlap of noise photon-counts from D1 and D3 within the time window of coincidence Δt, and the overlap of noise photon-counts of the detectors (D1 and D3, respectively) with the down-converted photons, then we have:

$$I_{1\text{ccNoise}} = N_1 N_3 \Delta t + I_{1\text{sync}} N_3 \Delta t + N_1 I_{1\text{signal}} \Delta t \tag{7}$$

where N_1 and N_3 are the numbers of noise photon-counts of D1 and D3, respectively. Then we have the readout number of coincidence of CC1:

$$I_{1\text{ccReadout}} = I_{1\text{cc}} + I_{1\text{ccNoise}} \tag{8}$$

By shrinking the time window of coincidence Δt to a few nanoseconds, $I_{1\text{ccNoise}}$ can be efficiently reduced, then $I_{1\text{ccReadout}} \approx I_{1\text{cc}}$, which means the readout number of CC1 is very close to the true value. The same goes for CC2.

In comparison, the readout number of D1, denoted as $I_{1\text{syncReadout}}$, is the sum of $I_{1\text{sync}}$ (the true value of photon-counts of D1) and $I_{1\text{Noise}}$ (the noise counts of D1). However, $I_{1\text{Noise}}$ of D1 can hardly be suppressed without the coincidence detection scheme, which causes the readout value of D1 to be inconsistent with the true value. Thus the result of Eq. (5) is more close to the true phase value than that of Eq. (4).

2.3. Experiment

2.3.1. Detector calibration

First, it is necessary to calibrate the efficiency of the detectors. The manufacturer claims that the quantum efficiency of SPCM-AQRH-16X is greater than 60% at 800nm. But the efficiency of each detector will vary. Since the measurement of absolute quantum efficiency η is more complicated, and the modified Eqs. (4) and (5), which are Eqs. (9) and (10) respectively, require only the measurement of the quantum efficiency ratio η_1/η_2 of D1 and D2, namely:

$$\alpha = \arccos\left(\sqrt{\frac{I_{1\text{sync}}}{I_{1\text{sync}} + \frac{\eta_1}{\eta_2} I_{2\text{sync}}}}\right) \tag{9}$$

or

$$\alpha = \arccos\left(\sqrt{\frac{I_{1\text{cc}}}{I_{1\text{cc}} + \frac{\eta_1}{\eta_2} I_{2\text{cc}}}}\right) \tag{10}$$

The specific calibration method uses D1 to measure the horizontally polarized photon flux (5 min), and denote the measured photon counts per second as I_{S1}; then uses D2 to measure the vertically polarized photon flow (5 min) and denote the obtained photon counts per second as I_{I2}. Then we exchange the detectors and repeat the process to get I_{S2} and I_{I1}, so we can obtain $\eta_1/\eta_2 = I_{S1}/I_{S2} = I_{I1}/I_{I2}$. After multiple measurements, the η_1/η_2 averages could be determined. For the following calculations in this article we use $(\eta_1/\eta_2) I_{2\text{sync}}$ and $(\eta_1/\eta_2) I_{2\text{cc}}$ to replace $I_{2\text{sync}}$ and $I_{2\text{cc}}$ in Eqs. (4) and (5), respectively.

Biomedical Optics EXPRESS

2.3.2. Selection of the principal axis of the λ/2 wave plate and wave plate calibration

WP2 is used to select the measurement base vectors**.** In the experiment, since the polarization plane of the beam only obtains a very small rotation, the highest sensitivity can be achieved by rotating the original horizontally polarized beam to a 45° linear polarization beam before reaching PBS3, so we should make the following equation true:

$$I_{1cc} \approx I_{2cc} \approx \frac{1}{2}(I_{1cc} + I_{2cc}) \tag{11}$$

If Eq. (11) holds, we have θ ≈ 45°, then after passing through the chiral solution, the angle goes to:

$$\alpha = 45^\circ - \alpha_T(t) \tag{12}$$

WP2 is calibrated before the measurement. The wave plate used in the experiment (PRM1/M from Thorlabs, USA) is a high-precision zero-order half wave plate. The phase retardation is π in the case of polarization in the principal axis direction with a wavelength of 808 nm, at a temperature of 20°C and a normal incidence. For the 800 nm wavelength, a correction factor of 808/800 should be multiplied for calculating the phase difference (without considering the dispersion between ordinary- and extraordinary-light). Then the angle θ (when $I_{1cc} \approx I_{2cc}$) must be accurately determined. We fill the sample cell with deionized water (the optical rotation of deionized water $\alpha_T(t)$ is assumed to be zero), and the angle θ is measured for 30 min. Following to Eq. (5), the precise value of θ and the corresponding random fluctuations are calculated, where a small deviation from the polarization angle of 45° is observed. By this procedure, the influence of the optical rotation of the quartz vessel on the measurement can also be effectively eliminated.

The laser power used for pumping entangled photons is around 10 mW, which produces about 4×10^6 photon pairs per second. The two SPDC photons are basically frequency-degenerate at 20°C, with a center wavelength of 800 nm and a bandwidth of 0.5 nm. The fibers coupled to D1, D2 and D3 are multimodal with the core diameter of 62.5μm. The coincidence count rates are maintained at about 13% throughout the whole measurement process (a total coincident count rate of 500,000 cps) with a coincidence time window of 3.2 ns in both CC1 and CC2. The sampling rate of the entire system is 1 sample/s.

3. Results and discussion

In a quartz chamber with a capacity of 5cm (length) × 4cm (height) × 1cm (width), 7.5mL different sucrose solutions with mass concentrations of 8% and 10% were added respectively. Each time, an additional 2.5 mL of 36% hydrochloric acid (diluted 1:3) is added to catalyze the hydrolysis of sucrose. The reaction process lasts for about 2 hours. As shown in Fig. 2., the rotation angle of the sucrose solution, which is $\alpha_T(t) = 45^\circ - \alpha$**,** is given by the quantum coincidence approach (Eq. (5)), where I_{cc} uses a 10-sec average value to make the curve smoother. The corresponding molar concentration of glucose with respect to reaction time obtained using Eqs. (1), (2), (3), and (5) is also presented in Fig. 2.

It is worth noting that the limited active collection area of the detectors (D1 and D2) combined with the photon-gathering multimode fibers (core diameter = 62.5μm, NA=0.22) poses challenges for our measurements of the liquid in contrast to solid-state samples. The operation of adding acid increases the flow of the liquid, which causes the light beam to shift and the collected photon-count to drop significantly. We wait 10 min for the solution to settle down, which means the starting point of the measurement ($t = 0$ min in Fig. 2.) is actually 10 min after the acid was added. When the sample settles down over a period of time, the light transmittance of the liquid slightly changes (~1%) during the measurement (due to the addition of hydrochloric acid, the sample is diluted), which is reflected in the change in the number of total coincidence counts. Around the moments $t = 60$ min and 100 min, we stirred the solution to ensure that the

Biomedical Optics EXPRESS

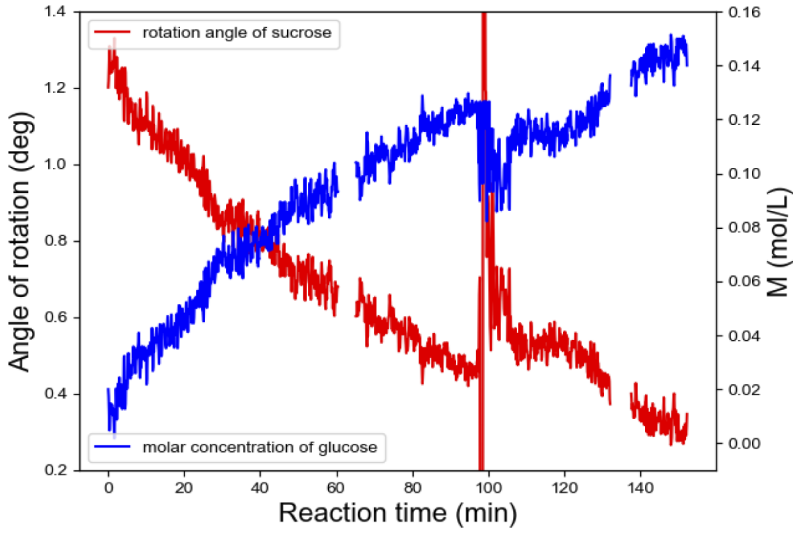

Fig. 2. Monitoring the rotation angle of the sucrose solution and molar concentration of glucose in the reaction process (the initial mass concentration of the sucrose solution is 8%).

reactant and catalyst were evenly mixed, which resulted in huge fluctuations in the number of coincidence-counts, and the calculated rotation angle of the solution exhibits a sharp peak around 100 min. We didn't show the peak at $t = 60$ min since it is very high and does not reflect the true phase angle.

Figure 3 reflects the situation where the reaction parameters can be continuously controlled. To simulate industrial biochemical reactions, hydrochloric acid is gradually added in the solution for the adjustment of reaction speed during the whole process. After the first addition of 2.5 mL hydrochloric acid, the reaction speed slows down significantly after 2 hours. Then another 1.5 mL hydrochloric acid (36%) is added. After another 2 hours' reaction, a final 2.5 mL is added. Thus, the reaction rate is adjusted by adding acid twice during the hydrolysis process. The total reaction time shown in Fig. 3 is 7 hours. After each addition of hydrochloric acid, the disturbed liquid scatters and deflects the probing light so much that the detectors can only collect part of the photons which are not in proportion. The unstable states last for 10~15 minutes, depending on the liquid's concentration and the filling speed of hydrochloric acid. This accounts for breaks in the plot in the above figure. After 10-15 min, the liquid becomes stable when the optical rotation angle can be accurately measured. After adding acid, the measurement parameters have to be adjusted, since the total molar concentrations of sucrose and glucose will decrease accordingly. Based on the new initial concentration values, we can monitor the biochemical reaction parameters such as the reaction rate through real-time measurements. The total molar concentration is reduced by nearly half by the end of the process.

Through calculation, we get the rotation angle-time curve for deionized water as shown in Fig. 4., which is performed before the sucrose hydrolysis experiment in order to accurately calibrate the angle θ [the angle between the principal axis of the $\lambda/2$ wave plate (WP2) and the horizontal direction]. As stated above, θ is preset to be 45° and the optical rotation of deionized water is considered to be 0. Using Eqs. (4), (5) and 10-sec average value of I_{sync} and I_{cc}, we get the standard deviations of α, which are $\sigma_{\text{single-photon counting}} = 0.0059°$ and $\sigma_{\text{coincidence counting}} = 0.0055°$ during the 37-minute period. It can be seen that the fluctuation of the photon-counts measured by coincidence method is slightly smaller than that of the classical one, but the number of coincidences measured is only one eighth of that of the classical measurement.

Biomedical Optics EXPRESS

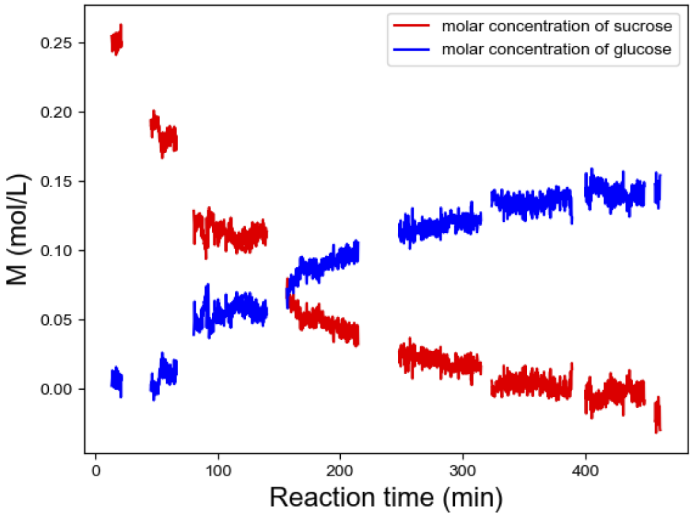

Fig. 3. Adjustment of the hydrolysis reaction rate of sucrose with an initial concentration of 10%.

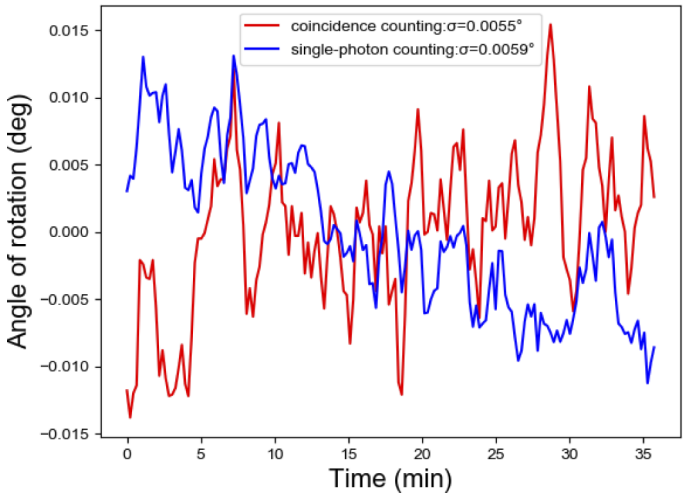

Fig. 4. Fluctuation of the optical rotation angle of the deionized water.

Biomedical Optics EXPRESS

However, the measurement approach in this work has no advantage in measurement accuracy and precision compared to a traditional polarimeter. The precision and angle resolution of our experiment are subject mainly to the generation rate of the SPDC photon pairs. The total coincidence count rate with a time window of 3.2 ns is $n_0 = 500{,}000$ cps (we use a 3.2 ns window because the dispersion of multimode fiber broadens our SPDC coincidence peak to a HWFM of 3.0 ns). According to [14], the precision of measured rotation angle $\Delta\alpha_T(t) \propto {I_0}^{-1/2}$, where $I_0 = n_0 T$, n_0 is the coincidence count rate and T is the integration time. When the integration time T=60s, the precision of the measured angle is less than 0.05 degree for a time span of several hours. Another factor that reduces the resolution is the polarizing beamsplitters used in our experiment has an extinction ratio of 1000:1, while an advanced polarimeter has a 1000,000:1 extinction ratio.

As demonstrated in Fig. 5., the coincidence counting method shows its insensitivity to the influence of environmental noise as compared with the single-photon counting measurement. This indicates that the quantum measurement can remain stable for a relatively long time during the hydrolysis process, whereas single-photon counting method fluctuates greatly with changes in ambient light (such as turning on and off lights).

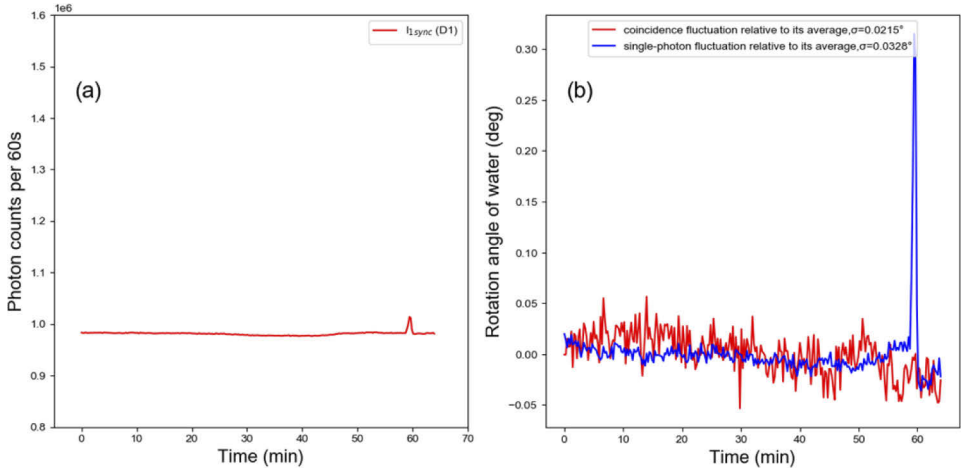

Fig. 5. The robustness of coincidence counting method compared with single-photon counting method. (a) An external light noise causes a small fluctuation of a number of 25,000 photon-counts on detector 1 ($I_{1\text{sync}}$) at around 60 min; (b) the single-photon counting method and coincidence counting method respond differently to the noise.

4. Conclusion

The quantum fluctuation of low-photon flux measurements (shot noise) is the main factor that compromises the signal-to-noise ratio and resolution of the experiment. The coincidence counting approach with quantum correlated photons can greatly reduce the noise influence introduced by the environment and the electronics, which is inaccessible to the classical single-photon counting method. This unique feature of coincidence detection makes it preferable in measuring some photosensitive bio-chemical reaction processes. The quantum method of measuring optical rotation that we introduce here is essentially an indirect measurement of the phase difference between left- and right-circularly polarized light when propagating with different refractive indexes in a chiral substance. Although the adoption of N00N states could improve the resolution of the measured phase angle [2,25], the method reported in this article still has its own advantages: (1) it has low requirements on the pump light source, the quality of the nonlinear crystal and

Biomedical Optics EXPRESS

light path adjustment in contrast to an interferometry approach. For instance, to obtain a higher coherent contrast N00N state, the spatial walk-off of the generated SPDC photons in the crystal has to be precisely compensated and single-mode fibers should be used to improve the light mode based on our existing light source; (2) it's less affected by the power, frequency, and mode-stability of the light source, as well as changes in ambient temperature. Therefore, the threshold for possible applications in the food and bioengineering industries will be correspondingly lower; (3) The accuracy of N00N states scheme relies heavily on the transmittance of the sample under test. A pre-calibration of the transmittance will be futile since it will change during the reaction (the sample will be diluted due to the addition of catalysts, and the transmittance changes consequently). For our scheme, the transmittance variation of the sample solution in the reaction process will not affect the measurement, since the number of vertically polarized photons varies in proportion to the horizontally polarized photons, so the calculated phase angle does not change.

Quantum metrology has broad applications in the fields of biological research and industrial productions. However, since most of the chiral molecules involved in biochemical reactions exist in aqueous solutions, the solution itself either strongly scatters photons, absorbs photons or changes the direction of the incident beam. Therefore, the efficient collection of photons becomes a problem. A promising solution would be to improve the quantum efficiency of the detector and increase the effective detection area. With the miniaturization and integration of quantum sensors on chips, quantum sensing technology is likely to quickly enter practical applications in the future.

Funding. ENN Research Fund (EIST202008).

Acknowledgments. This work is supported by ENN Research Fund (Grant No. EIST202008) and Hebei Key Laboratory of Health Monitoring and Evaluation. At the same time, the authors would like to thank H. H. Su and Y. J. Chen for providing solution samples.

Disclosures. The authors declare no potential conflict of interests.

Data availability. Data underlying the results presented in this paper are not publicly available at this time but may be obtained from the authors upon reasonable request.

References

1. L. D. Barron, *Molecular Light Scattering and Optical Activity*, 2nd ed. (Cambridge University, 2004).
2. V. Cimini, M. Mellini, G. Rampioni, M. Sbroscia, L. Leoni, M. Barbieri, and I. Gianani, "Adaptive tracking of enzymatic reactions with quantum light," Opt. Express **27**(24), 35245–35256 (2019).
3. H. Mirmiranpour, F. S. Nosrati, S. O. Sobhai, S. N. Takantape, and A. Amjadi, "Effect of low-level laser irradiation on the function of glycated catalase," J. Lasers Med. Sci. Summer **9**(3), 212–218 (2018).
4. G. I. Klebanov and M. V. Kreinina, "Free-radical mechanism of photobiological effect of low-level laser irradiation," Proc. SPIE **4422**, 30 (2001).
5. Y. M. Blanter and M. Büttiker, "Shot noise in mesoscopic conductors," Phys. Rep. **336**(1-2), 1–166 (2000).
6. F. Lefloch, C. Hoffmann, M. Sanquer, and D. Quirion, "Doubled full shot noise in quantum coherent superconductor-semiconductor junctions," Phys. Rev. Lett. **90**(6), 067002 (2003).
7. A. A. Kozhevnikov, R. J. Schoelkopf, and D. E. Prober, "Observation of photon-assisted noise in a diffusive normal metal–superconductor junction," Phys. Rev. Lett. **84**(15), 3398–3401 (2000).
8. E. Jakeman and J. G. Rarity, "The use of pair production processes to reduce quantum noise in transmission measurements," Opt. Commun. **59**(3), 219–223 (1986).
9. M. M. Hayat, A. Joobeur, and B. E. A. Saleh, "Reduction of quantum noise in transmittance estimation using photon-correlated beams," J. Opt. Soc. Am. A **16**(2), 348–358 (1999).
10. C. K. Hong, S. R. Friberg, and L. Mandel, "Optical communication channel based on coincident photon pairs," Appl. Opt. **24**(22), 3877–3882 (1985).
11. D. A. Kalashnikov, Z. Pan, A. I. Kuznetsov, and L. A. Krivitsky, "Quantum spectroscopy of plasmonic nanostructure," Phys. Rev. X **4**(1), 011049 (2014).
12. V. Giovannetti, S. Lloyd, and L. Maccone, "Advances in quantum metrology," Nat. Photonics **5**(4), 222–229 (2011).
13. V. Giovannetti, S. Lloyd, and L. Maccone, "Quantum-enhanced measurements: Beating the standard quantum limit," Science **306**(5700), 1330–1336 (2004).
14. M. A. Taylor and W. P. Bowen, "Quantum metrology and its application in biology," Phys. Rep. **615**, 1–59 (2016).
15. M. A. Taylor, J. Janousek, V. Daria, J. Knittel, B. Hage, H. Bachor, and W. P. Bowen, "Biological measurement beyond the quantum limit," Nat. Photonics **7**(3), 229–233 (2013).

Biomedical Optics EXPRESS

16. G. B. Lemos, V. Borish, G. D. Cole, S. Ramelow, R. Lapkiewicz, and A. Zeilinger, "Quantum imaging with undetected photons," Nature **512**(7515), 409–412 (2014).
17. I. Kviatkovsky, H. M. Chrzanowski, E. G. Avery, H. Bartolomaeus, and S. Ramelow, "Microscopy with undetected photons in the mid-infrared," Sci. Adv. **6**(42), 264 (2020).
18. M. B. Nasr, D. P. Goode, N. Nguyen, G. Rong, L. Yang, B. M. Reinhard, B. E. A. Saleh, and M. C. Teich, "Quantum optical coherence tomography of a biological sample," Opt. Commun. **282**(6), 1154–1159 (2009).
19. A. V. Paterova, H. Yang, Ch. An, D. A. Kalashnikov, and L. A. Krivitsky, "Polarization effects in nonlinear interference of down-converted photons," Opt. Express **27**(3), 2589–2603 (2019).
20. D. A. Kalashnikov, A. V. Paterova, S. P. Kulik, and L. A. Krivitsky, "Infrared spectroscopy with visible light," Nat. Photonics **10**(2), 98–101 (2016).
21. A. V. Paterova, S. Lung, D. A. Kalashnikov, and L. A. Krivitsky, "Nonlinear infrared spectroscopy free from spectral selection," Sci. Rep. **7**(1), 42608 (2017).
22. A. V. Paterova, H. Z. Yang, C. W. An, D. A. Kalashnikov, and L. A. Krivitsky, "Measurement of infrared optical constants with visible photons," New J. Phys. **20**(4), 043015 (2018).
23. A. V. Paterova, S. M. Maniam, H. Yang, G. Grenci, and L. A. Krivitsky, "Hyperspectral infrared microscopy with visible light," Sci. Adv. **6**(44), eabd0460 (2020).
24. N. Tischler, M. Krenn, R. Fickler, X. Vidal, A. Zeilinger, and G. Molina-Terriza, "Quantum optical rotatory dispersion," Sci. Adv. **2**(10), e1601306 (2016).
25. V. Cimini, I. Gianani, L. Ruggiero, T. Gasperi, M. Sbroscia, E. Roccia, D. Tofani, F. Bruni, M. A. Ricci, and M. Barbieri, "Quantum sensors for dynamical tracking of chemical processes," Phys. Rev. A **99**(5), 053817 (2019).
26. A. Penzkofer, "Optical rotatory dispersion measurement of d-glucose with fixed polarizer analyzer accessory in conventional spectrophotometer," J. Analyt. Sci., Methods Instr. **3**, 234–239 (2013).
27. S. M. Mahurin, R. N. Compton, and R. N. Zare, "Demonstration of optical rotatory dispersion of sucrose," J. Chem. Educ. **76**(9), 1234–1236 (1999).